COMMUNICATIONS IN COMPUTATIONAL PHYSICS
Vol. **1**, No. 1, pp. 81-99

Commun. Comput. Phys.
February 2006

Chaotic Driven Tunneling in Rectangular Double-Well

V. L. Golo[1,*] and Yu. S. Volkov[1]

[1] *Department of Mechanics and Mathematics, Moscow State University, Moscow 119 899 GSP-2, Russia.*

Received 20 July 2005; Accepted (in revised version) 9 August 2005

Communicated by Dietrich Stauffer

Abstract. We consider a charged particle confined in a one-dimensional rectangular double-well potential, driven by an external periodic excitation at frequency Ω and with amplitude A. We find that there is the regime of the parametric resonance due to the modulation of the amplitude A at the frequency ω_{prm}, which results in the change in the population dynamics of the energy levels. The analysis relies on the Dirac system of Hamiltonian equations that are equivalent to the Schrödinger equation. Considering a finite dimensional approximation to the Dirac system, we construct the foliation of its phase space by subsets $\mathcal{F}_{ab}$ given by constraints $a \leq N_0 \leq b$ on the occupation probabilities N_0 of the ground state, and describe the tunneling by frequencies ν_{ab} of the system's visiting subsets $\mathcal{F}_{ab}$. The frequencies ν_{ab} determine the probability density and thus the Shannon entropy, which has the maximum value at the resonant frequency $\omega = \omega_{prm}$. The reconstruction of the state-space of the system's dynamics with the help of the Shaw-Takens method indicates that the quasi-periodic motion breaks down at the resonant value ω_{prm}.

Key words: Tunneling; double-well; parametric resonance.

1 Introduction: Tunneling in the finite dimensional Hamiltonian approximation

Driven transitions in a double well are instrumental for studying the tunneling in various fields of physics and chemistry, [1,2]. Considerable attention has been drawn to the tunneling dynamics in the presence of a driving force with a time dependent amplitude. In his seminal paper [3], M. Holthaus showed that shaping the driving force may be instrumental in controlling the tunneling in a bistable potential. In particular, it was shown, [3], that choosing an appropriate envelope for laser pulse, one may perform the population transfer on time scales much shorter than the

*Correspondence to: V.L. Golo, Department of Mechanics and Mathematics, Moscow State University, Moscow 119 899 GSP-2, Russia. Email: golo@mech.math.msu.su

base tunneling time. This situation is intimately related to the problem of quantum chaos, which is generally approached within the framework of the quasi-classical approximation and Gutzwiller's theory. In fact, classical chaotic systems are often used as a clue to the quantum ones. In contrast, it would be very interesting to look at the quantum chaos the other way round and consider systems which need studying without approximations that could have bearing upon classical mechanics, for example, particles confined to potentials of a size comparable with the de Broglie wave length. This has also an additional interest owing to the fact that calculations within the framework of semiclassical theory should depart from the quantum ones on the time scale of $\hbar/\Delta E$, ΔE being the typical spacing between energy levels. Specifically, the Schrödinger equation describing the problem needs numerical studying.

The current approach to the tunneling generally focuses on localization of wave packets, and uses the concept of dwell time. The latter is usually taken in the form, [4, 5],

$$\tau_D(a,b) = \int_{-\infty}^{+\infty} dt \int_a^b |\psi(x,t)|^2 \, dx. \tag{1.1}$$

Even though the concept of dwell time is generally recognized as an important characteristic of the wave packet, [6], it brings forward conceptual difficulties owing to the special role played by time in quantum mechanics, [6, 7]. Consequently, it is often difficult to determine a quantity that should be both correct and practical for studying the tunneling dynamics in a double well potential, if we wish to describe the particle's localization in one of the potential wells. Fortunately, in certain cases the choice of the well really means the choice of an energy state, as illustrated in Fig. 1, and consequently there is an opportunity for considering the tunneling dynamics in the energy representation, instead of the x-one. To put it in a quantitative form, let us consider the characteristic function $\chi_{ab}(x)$ which is 1 if $a \le x \le b$ and 0 otherwise, and introduce the quantity

$$\nu_\phi(a,b) = \lim_{T\to\infty} \left\{ \frac{1}{T} \int_{-T/2}^{+T/2} \chi_{ab}(N_\phi)\, dt \right\}, \qquad N_\phi = |<\psi|\phi>|^2, \tag{1.2}$$

where $\psi(t)$ is a solution of the Schrödinger equation, and ϕ is a state of the system.

The time averaged probability $\nu_\phi(a,b)$ can be visualized as the frequency of visiting a region of states determined by constraint $a \le N_\phi \le b$. It is easy to see that (1.2) is similar to (1.1), $\nu_\phi(a,b)$ describing the system's dwell time in segment (a,b). At first sight, the calculation of $\nu_\phi(a,b)$ looks rather complicated, and in fact the direct numerical integration of the Schrödinger equation is time consuming and requires special precautions to overcome possible artifacts. However, to solve the problem one may use the method proposed by Dirac [8] for studying the interaction of an atomic system with radiation. It relies on the decomposition of the system's Hamiltonian

$$H = H_0 + V,$$

where H_0 is the main term, and V is the term describing the interaction with external field. If

$\psi(x,t)$ is a solution to the Schrödinger equation

$$i\hbar\frac{\partial\psi}{\partial t} = H\psi, \tag{1.3}$$

we may cast $\psi(x,t)$ in the form of series

$$\psi(x,t) = \sum_n c_n\,\psi_n(x,t), \tag{1.4}$$

where coefficients c_n depend on time, indices n may have continuous values, [8], and $\psi_n(x,t)$ are stationary solutions to (1.3) with the integration term, H_1, being cancelled out,

$$\psi_n(x,t) = \exp\left(\frac{-iE_n}{\hbar}t\right)\phi_n.$$

The coefficients c_n verify the equations

$$i\hbar\,\partial_t\,c_n = \sum_m V_{nm}\,c_m, \qquad V_{nm} = \exp\left(i\frac{E_n - E_m}{\hbar}t\right) < \phi_n|V|\phi_m > \tag{1.5}$$

which are the Hamiltonian ones, as can be seen from the fact that

$$i\hbar\,\partial_t\,c_n = \{c_n, F\}$$

where the Poisson bracket $\{,\}$ and Hamiltonian F are defined by the equations

$$\{c_n^*,\, c_m\} = i\,\delta_{nm}, \qquad F = \sum_{nm} c_n^*\,V_{nm}\,c_m.$$

Thus, $c_0, c_1, \ldots, c_n, \ldots; c_0^*, c_1^*, \ldots, c_n^*, \ldots$ form the phase space of the Hamiltonian system given by (1.5), which is equivalent to the initial Schrödinger equation. The occupation probabilities for $\psi_k(x,t)$ as regards to $\psi(x,t)$ read

$$N_k = c_k^* c_k = |\,<\psi|\phi_k>\,|^2.$$

We are mainly interested in the ground state and the occupation probability N_0. To this end, consider the foliation of the phase space given by the sets

$$\mathcal{F}_{k\,k+1} \qquad \Delta_k \le N_0 \le \Delta_{k+1}, \qquad k = 1,2,3,\ldots,\mathcal{N},$$

where Δ_k are intervals dividing segment (0,1) in $\mathcal{N}$ equal parts.

For the ground state of the system ϕ_0 we use the short notation $\nu_{ab} = \nu_{\phi_0}(a,b)$. The visiting frequencies in the short notation

$$\nu_{k\,k+1}$$

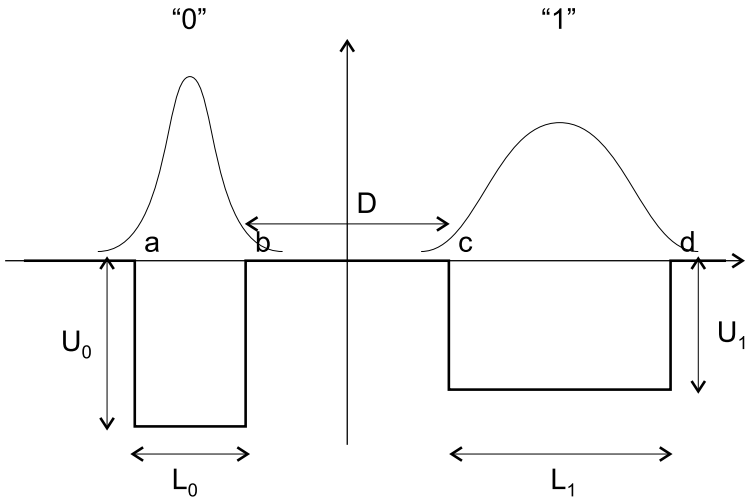

Figure 1: Rectangular one-dimensional double-well potential. Lines "0" and "1" indicate the moduli of the wave functions $|\psi_0(x,t)|$ and $|\psi_1(x,t)|$ of the ground and the first excited states, respectively. D is the distance between the wells; L_0, L_1 and U_0, U_1 are the widths and depths of the wells.

are defined by the time τ_k spent by the trajectory in $\mathcal{F}_{k\,k+1}$ (see, Fig. 2). By considering the ratios

$$\rho(N_0) = \frac{\nu_{k\,k+1}}{\Delta_{k+1} - \Delta_k} = \frac{\nu_\Delta}{\Delta} \tag{1.6}$$

we obtain a coarse-grained probability distribution for N_0, for the chosen period of time T. It turns out, see Section 4 for the details, that the right hand side of (1.6) tends to a limit as $T \to \infty$. By letting $\Delta \to 0$ we obtain the probability density, $\rho(N_0)$, for the distribution of N_0. Hence, we may define the Shannon entropy

$$\sigma = -\int \rho \ln \rho \, dN_0$$

which is "a measure of the amount of uncertainty represented by a probability distribution", see, e.g., [9]. The entropy σ, which is determined by the external field and in particular the parametric excitation, turns out to be a valuable numerical means for studying the character of the tunneling dynamics.

Thus the Hamiltonian system obtained with the Dirac equations serves as the instrument both for the numerical solution of the Schrödinger equation and for the qualitative analysis of the tunneling. Last but not least, we may employ the Cranck-Nicholson finite difference method as an alternative way of numerically solving the Schrödinger equation, which provides a valuable test of our calculations.

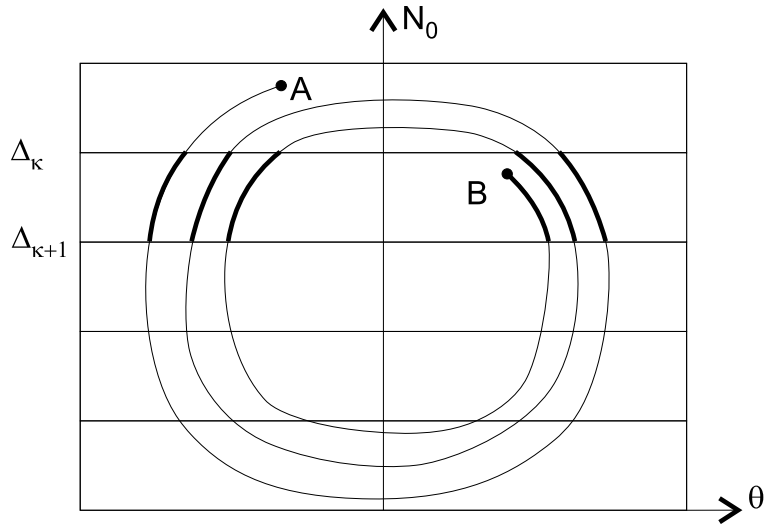

Figure 2: Intersection of a trajectory with the region in the phase-space determined by the relation $\Delta_k \leq N_0 \leq \Delta_{k+1}$ in $(N_0 - \theta)$ window, $\theta = \phi_1 - \phi_0$, where ϕ_0, ϕ_1 are the phases of the complex quantities c_0, c_1

2 Transition frequencies of the driven tunneling

We shall consider a particle confined in the rectangular potential of the form, see Fig. 1,

$$U = \begin{cases} -U_0, & a \leq x \leq b \\ -U_1, & c \leq x \leq d \\ 0, & \text{otherwise} \end{cases} \tag{2.1}$$

where a, b, c, d together with U_0, U_1 are used here as the exact parameters of the potential configuration. The particle is considered under the action of an external field, corresponding to an electromagnetic wave, given in the x-representation by the equation

$$V = A \sin \Omega t \left(-i\hbar \frac{\partial}{\partial x} \right) \tag{2.2}$$

so that the particle's dynamics is determined by the Schrödinger equation

$$i\hbar \frac{\partial}{\partial t} \psi = -\frac{\hbar^2}{2m} \frac{\partial^2}{\partial x^2} \psi + U(x)\psi + V(x,t)\psi. \tag{2.3}$$

The stationary solutions to (2.3) without external field $V(x,t)$ are assumed to be known.

The perturbation or excitation potential can be visualized as the vector potential of a monochromatic wave. We may cast the solution in the form of (1.4), in which the continuous part of the spectrum is accommodated with continuous indices n, see, e.g., [8]. Thus the

problem of finding a solution to the Schrödinger equation is reduced to that of solving the Hamiltonian system given by (1.5); at this point it should be noted that (1.5) is equivalent to the initial Schrödinger equation. Therefore, it is not easier than the latter, but, it admits approximations for its solution. In this paper, we shall consider only bound states and neglect the continuous part of the spectrum so that the sum in n of (1.5) be finite. We may use a finite dimensional approximation to the infinite system (1.5), which is equivalent to the Galerkin method for solution of ordinary differential equations.

We choose the parameters of the double-well potential in such a way that the ground state of the particle be almost totally confined in one well, and the first excited one in another.

In what follows we shall denote the transition frequencies and the matrix elements of the excitation potential by

$$\omega_{nm} = (E_n - E_m)/\hbar, \quad \text{and} \quad V_{nm} = A \sin\Omega t \, \exp(i\alpha_{nm}) \, \kappa_{nm}$$

where κ_{nm} is the modulus of the matrix element and α_{nm} is the phase (see (1.5)).

A qualitative description of the transitions between the ground state and the first excited state can be obtained by employing the rotating wave approximation [10] in the following manner. First, we neglect the whole energy levels, besides the first two, so that the equations take the form

$$\begin{aligned} i\hbar\,\partial_t\, c_0 &= A \sin\Omega t \, \exp(-i(\omega_{10}t + \alpha))\kappa \, c_1 \\ i\hbar\,\partial_t\, c_1 &= A \sin\Omega t \, \exp(i(\omega_{10}t + \alpha))\kappa \, c_0 \end{aligned}$$

where $\alpha = \alpha_{10}$ and $\kappa = \kappa_{10}$. By considering the resonance case $\Omega = \omega_{10}$ and neglecting all oscillating terms we cast the equations of motion in the matrix form

$$i\hbar\,\partial_t\,\vec{c} = M\,\vec{c}, \tag{2.4}$$

where $\vec{c} = (c_0(t), c_1(t))$ and

$$M = \frac{A\kappa}{2}\,(-\sin\alpha\,\sigma_1 + \cos\alpha\,\sigma_2).$$

In the above equation, σ_1, σ_2 are the Pauli matrices

$$\sigma_1 = \begin{pmatrix} 0 & 1 \\ 1 & 0 \end{pmatrix}, \qquad \sigma_2 = \begin{pmatrix} 0 & -i \\ i & 0 \end{pmatrix}.$$

Using the transformation

$$\vec{c} = U\,\vec{d}, \qquad U = \begin{pmatrix} \exp(-i\alpha/2) & 0 \\ 0 & \exp(i\alpha/2) \end{pmatrix},$$

we cast the equation given above in the form

$$i\hbar\,\partial_t\,\vec{d} = \frac{A\kappa}{2}\,\sigma_2\,\vec{d}. \tag{2.5}$$

The equation describes the transitions between the energy levels $|0>$, $|1>$ due to the resonance $\Omega = (E_1 - E_0)/\hbar$. The frequency of transitions between levels $|0>$, $|1>$ reads

$$\nu = \frac{A\kappa}{2\hbar}.$$

Now let us consider the parametric excitation given by

$$A = A_0\,(1 - \epsilon\,\sin\omega t). \tag{2.6}$$

Following the Rayleigh argument, [11], it can be verified that there is a parametric resonance at the frequency

$$\omega = \omega_{prm} = \frac{A_0\kappa}{\hbar}$$

that is two times larger than the frequency of the usual resonance.

To see the physical picture of the tunneling we transform from the variables c_n, c_n^* to the occupation probabilities N_k and phases ϕ_k by the canonical transformation

$$c_n = \sqrt{N_k}\,\exp(i\phi_k)$$

so that the following equations for Poisson brackets are true, [8],

$$\{N_k, N_m\} = 0, \quad \{\phi_k, \phi_m\} = 0, \quad \{\phi_m, N_k\} = \delta_{km}. \tag{2.7}$$

Consequently, the Hamiltonian F reads

$$F = A\,\sin(\Omega t)\,\sum_{mn}\,\kappa_{mn}\,\sqrt{N_m N_n}\,\exp(-i(\omega_{mn}t - \phi_m + \phi_n - \alpha_{mn})) \tag{2.8}$$

Therefore, the Dirac equation is a Hamiltonian system with the phase-space determined by the conjugate variables

$$N_0, N_1, \ldots, N_k \ldots; \phi_0, \phi_1, \ldots, \phi_k, \ldots,$$

The finite Hamiltonian approximation to the system determined by the Poisson brackets indicated above, is obtained by considering only variables with indices less or equal to the number of bound states. There have been a number of approaches to describing the dynamics of solutions to the Schrödinger equation, see [14], for example the Humishi phase space density

$$\rho(p, q, t) = |< p, q|\psi_{p_0,q_0(t)}>|^2$$

in which the dynamics of an initial coherent state $|\psi_{p_0,q_0(t=0)}>$, where $|p, q>$ is a coherent state determined by values of p, q. In this paper we are using a similar quantity but employ eigenfuctions of energy levels.

The general picture of the tunneling dynamics in the specific case we are considering, can be visualized through the use of variables $N_0 = c_0^* c_0$, the occupation probability of the ground state, and $\theta = \phi_1 - \phi_0$, the phase shift of the phase of the ground state and the first excited level.

It is important that there is a double resonance; the first one at frequency $\Omega = (E_1 - E_0)/\hbar$ corresponding to the transition from the ground state to the next level, and the second one due to the parametric excitation at frequency $\omega = \omega_{prm} = A_0\kappa_{10}/\hbar$, and the frequency of the parametric resonance is much smaller than the transition frequency Ω owing to small amplitudes of the excitation A_0 and the modulus κ_{10} of V_{10}. The parametric excitation in the resonance regime is illustrated in Fig. 9. We see that it changes considerably the dynamics of the tunneling. The collapse of the peaks, which are characteristic of the driven tunneling without the parametric excitation, agrees with the existence of the peak, see Fig. 10, of the entropy $\sigma(\omega)$ considered as the function of the parametric excitation frequency ω in (2.6).

We may study the dynamics of the system by employing the two-dimensional window on the phase space formed by the pair of variables N_0, θ, in which $\theta = \phi_1 - \phi_0$. It is worth noting that Dirac's equations can be written down with the help of the variables N_k, $\theta_{kl} = \phi_k - \phi_l$, $k, l = 1, 2, 3, \ldots$ in the form of Poisson brackets with Hamiltonian

$$\partial_t N_m = \{N_m,\, F\},\ \partial_t \theta_{kl} = \{\theta_{kl},\, F\}.$$

We may obtain the two level approximation used above by employing the variables N_0, $\theta = \theta_{01}$, instead of c_0, c_1. Suppose that there is only the resonance

$$\Omega = \frac{1}{\hbar}\,(E_1 - E_0).$$

Let us neglect N_i for $i > 1$ and θ_{kl} for $k \quad \text{or} \quad l > 1$, and preserve only the resonance terms in the equations of motion indicated above.

$$\begin{aligned} \partial_t N_0 &= A\kappa\sqrt{N_0 N_1}\cos(\theta + \alpha), \\ \partial_t N_1 &= -A\kappa\sqrt{N_0 N_1}\cos(\theta + \alpha), \\ \partial_t \theta &= -A\kappa\frac{N_1 - N_0}{\sqrt{N_0 N_1}}\sin(\theta + \alpha). \end{aligned} \tag{2.9}$$

Note that from the above equations we have $N_0 + N_1 = \text{const}$ or owing to the chosen approximation $N_0 + N_1 = 1$. Thus we may cast the equations in the form

$$\begin{aligned} \partial_t N_0 &= A\kappa\sqrt{N_0(1 - N_0)}\cos(\theta + \alpha), \\ \partial_t \theta &= -A\kappa\frac{1 - 2N_0}{\sqrt{N_0(1 - N_0)}}\cos(\theta + \alpha), \end{aligned}$$

which is equivalent to (2.4).

Thus, we obtain the rotating wave approximation, [10], which is a 2-dimensional approximation to the exact Hamiltonian system of Dirac's equations. We may utilize the variables N_0, θ employed above for constructing a 2-dimensional window on the phase space of Dirac's equations. For this end, we shall consider solutions to the Dirac equations truncated up to the six energy levels, which correspond to the six bound states of our two-well potential, and take their projections $N_0(t), \theta(t)$ at the moment of time t in plane $N_0\theta$. The picture we obtain in this

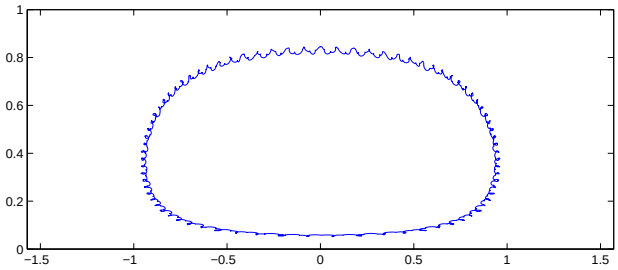

Figure 3: Phase picture in 2-d $N_0 - \theta$ window on Dirac's system. Resonance amplitude $A_0 = 0.3$, no parametic excitation. Initial position trajectory: $N_0 = 0.9191$, $N_1 = 0.3939$, $N_i = 0$, $i \geq 2$; the system initial state is a mixture of the first two states.

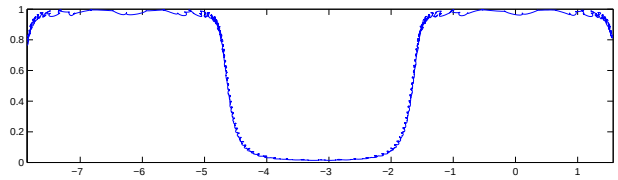

Figure 4: Phase picture in 2-d $N_0 - \theta$ window on Dirac's system. Separaterixe solution. Resonance amplitude $A_0 = 0.3$, no parametic excitation. Initial position trajectory: $N_0 = 0.9137$, $N_1 = 0.4062$, $N_i = 0$, $i \geq 2$; $\theta = \pi/2$. The system initial state is a mixture of the first two states.

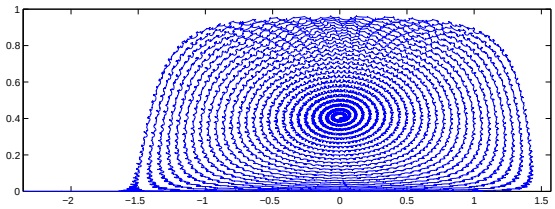

Figure 5: Phase picture in 2-d $N_0 - \theta$ window on Dirac's system. The trjectory corresponds to the breakdown of the periodic solution. Resonance amplitude $A_0 = 0.3$, $\epsilon = 0.1$, the frequency 0.01690. Initial position trajectory: $N_0 = 0.6332$, $N_1 = 0.7739$, $N_i = 0$, $i \geq 2$; the system initial state is a mixture of the first two states.

way, strongly depends on the form of the excitation potential V given by (2.6). In case there is no parametric excitation, that is the amplitude A is constant, the rotating wave approximation is good enough and its phase picture agrees with that obtained through the 2-dimensional $N_0\theta$ window on Dirac's system, see Figs. 3-4.

The dynamics drastically changes in case there is the parametric excitation at the resonance

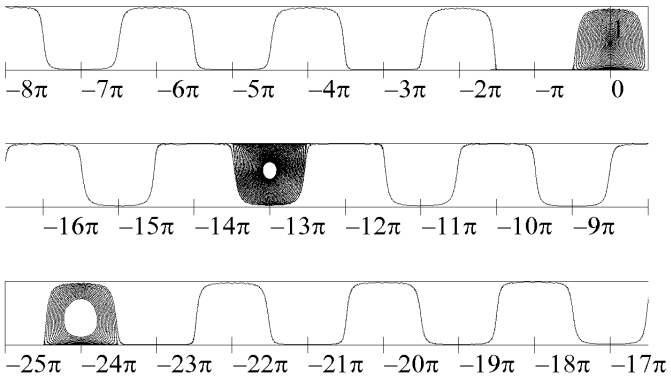

Figure 6: Phase picture in 2-d $N_0 - \theta$ window on Dirac's system. The trjectory corresponds to the breakdown of the periodic solution. Resonance amplitude $A_0 = 0.3$, $\epsilon = 0.1$, the frequency 0.01690. Initial position trajectory: $N_0 = 0.6332$, $N_1 = 0.7739$, $N_i = 0$, $i \geq 2$; the system initial state is a mixture of the first two states.

frequency ω_{prm}

$$A(t) = A_0 \left(1 - \epsilon \, \sin \omega_{prm} t\right)$$

as is shown in Figs. 5-6.

In fact, the width, W (see Fig. 7), of the stripe spanned by the trajectory in plane $N_0 - \theta$ is the maximal one in the resonance regime. Therefore, on considering the width W against the frequency ω of the parametric excitation, we obtain a graphic description of the onset of the resonance. As is shown in Fig. 8, the resonance has a fine structure given by the presence of two peaks, close to each other.

The fine structure is important for numerical modelling the parametric resonance, for by choosing $\omega = \omega_{min}$, where ω_{min} corresponds to the minimum of W, we get into the region inside which the resonance is to all purposes absent.

During the period of time T a trajectory of the approximate system spends the time τ_n in the set $\mathcal{F}_{nn+1}$. The time can be found by considering the trajectory in plane $(N_0 - \theta)$, where $\theta = \phi_1 - \phi_0$, see Fig. 2. We obtain in this way a coarse-grained probability distribution on the phase space of the approximate system, and therefore an approximate probability distribution for the quantum problem. It should be noted that the averaging procedure given above by (1.6) is correct, as can be seen by comparing the averages for various large values of the period of time T, see Fig. 13.

3 Visualization

The visualization of the tunneling dynamics relies on Dirac's equations, which give an equivalent Hamiltonian formulation of the Schrödinger equation, and comprises the two steps. First, we use the $(N_0 - \theta)$ window on the phase space of Dirac's equations, see Figs. 5 - 6, and obtain a

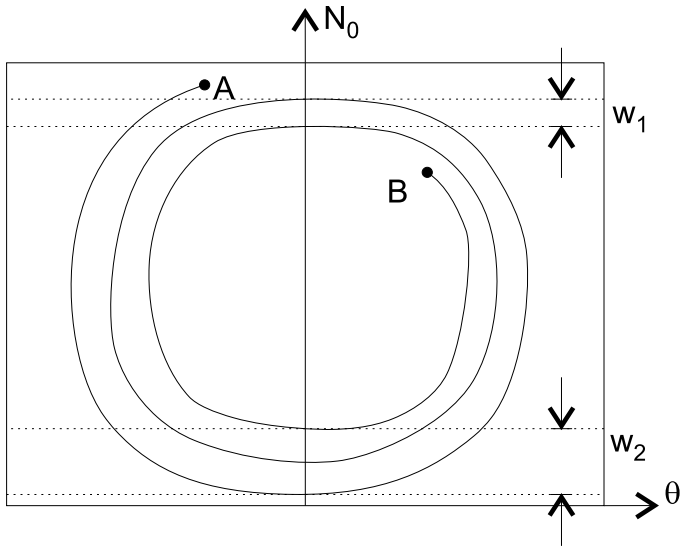

Figure 7: Width of the stripe spanned by the trajectory in $(N_0 - \theta)$ window consists of two halves - w_1 and w_2, top and bottom respectively, which are calculated by considering intersections of a trajectory with axis N_0. Full width $W = w_1 + w_2$.

graphic picture of the onset of the parametric resonance, as well as a means for its quantitative analysis. Second, we use the Shaw-Takens method, [13], for the visualizing the state-space of a dynamical system. For this end, we consider a variable X characteristic of the system, and form a time series that comprises the values of X at moments of time $\tau n, \quad n = 0, 1, 2, \ldots$, τ being the lag-time, so that

$$X_0 = X(0), X_1 = X(\tau), X_2 = X(2\tau), \ldots, X_k = X(k\tau), \ldots$$

Next, we consider the series of vectors

$$Y_0 = (X_0, X_1, \ldots, X_d), \quad Y_1 = (X_1, X_2, \ldots, X_{d+1}), \ldots$$

According to the general belief, points $Y_0, Y_1, Y_2, \ldots, Y_k, \ldots$ of d-dimensional space form a set that serves a visualization of the state-space for the given problem. It is to be noted that the final outcome depends on a number of premises, and first of all on the value of the time-lag τ and the dimension d of the visualization window. The wise choice of τ is dictated by characteristic times of the motion under the investigation, so that for certain values of τ the visualization picture is coherent enough whereas for others it is not meaningful. Therefore, using the Shaw-Takens method one has to compare pictures obtained for different values of the lag-time.

In this paper we are applying the Shaw-Takens method to: (1) the tunneling dynamics in the presence of a parametric excitation, and (2) in the absence of the latter. For the last, there is obtained the picture of a torus in 3d-space, fairly well drawn, without sudden modifications due

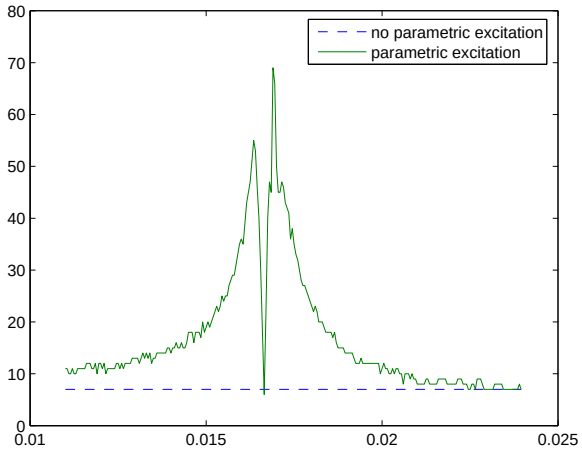

Figure 8: Width of the stripe against the excitation frequency (in procents of maximum width). The line at the bottom shows the width value in the absence of the parametric resonance. The maximum at $\omega = \omega_{prm} = 0.01690$ corresponding to the peak of Fig. 10. Resonance amplitude $A_0 = 0.3$, $\epsilon = 0.1$. Initial conditions for the entropy curve are $N_0 = 0.8320$, $N_1 = 0.5547$, $N_i = 0$, $i \geq 2$; the system initial state is a mixture of the first two states.

to changes in the lag-time, but only continuos deformations of the initial picture. In contrast, if the parametric excitation at the resonant frequency is present, the choice of the lag-time is very important for obtaining a meaningful visualization. There is a tendency of suddenly changing the shape of the visualization owing to the choice of the lag-time, see Fig. 11.

In particular, we obtain the visualization of the state-space of two kinds. The first one has the shape of a cloud with an inside blurred nucleus whose structure is not clear. The second one has the shape of tangled pipes of various diameter and irregularly located. The change of the lag-time is accompanied by a transition from the first one to the second, and vice versa.

4 Numerical modelling

The study of the parametric resonance even for the simplest model given by the rotating wave approximation requires the use of numerical simulation. The situation becomes even more complicated when one tries to accommodate the neglected terms and higher frequency oscillations, which substantially influence the tunneling dynamics. At this point it is worthwhile to note that we take into account the bound states and neglect the continuous part of the spectrum.

The Dirac equations without any simplifications and approximations, read

$$i\hbar\,\partial_t\,c_k = A\,\sin\Omega t\,\sum_m \exp(i[\frac{(E_n - E_m)}{\hbar}t + \alpha_{nm}])\,\kappa_{nm}\,c_m \tag{4.1}$$

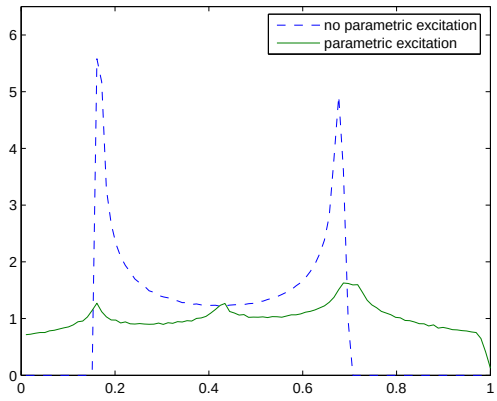

Figure 9: Probability density $\rho(N_0)$ for the distribution of N_0 with $A_0 = 0.3$; 6 six bound states (levels confined to the well). Dashed line - no parametric excitation. Solid line - parametric excitation, $\epsilon = 0.1$, parametric frequency $\omega = \omega_{prm} = 0.01690$. Initial conditions for both distributions are $N_0 = 0.8320$, $N_1 = 0.5547$, $N_i = 0$, $i \geq 2$; the system initial state is a mixture of the first two states.

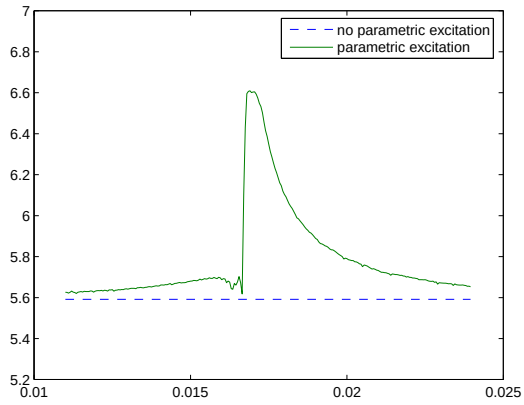

Figure 10: Entropy σ against the frequency ω of the parametric excitation. The line at the bottom shows the entropy value in the absence of the parametric resonance. The maximum at $\omega = \omega_{prm} = 0.01690$ corresponding to the second peak of Fig. 8. Resonance amplitude $A_0 = 0.3$, $\epsilon = 0.1$. Initial conditions for the entropy curve are $N_0 = 0.8320$, $N_1 = 0.5547$, $N_i = 0$, $i \geq 2$; the system initial state is a mixture of the first two states.

The first question to be resolved is how many terms on the rhs we shall take to obtain a meaningful approximation. The answer depends on the size of the potential well, especially its depth.

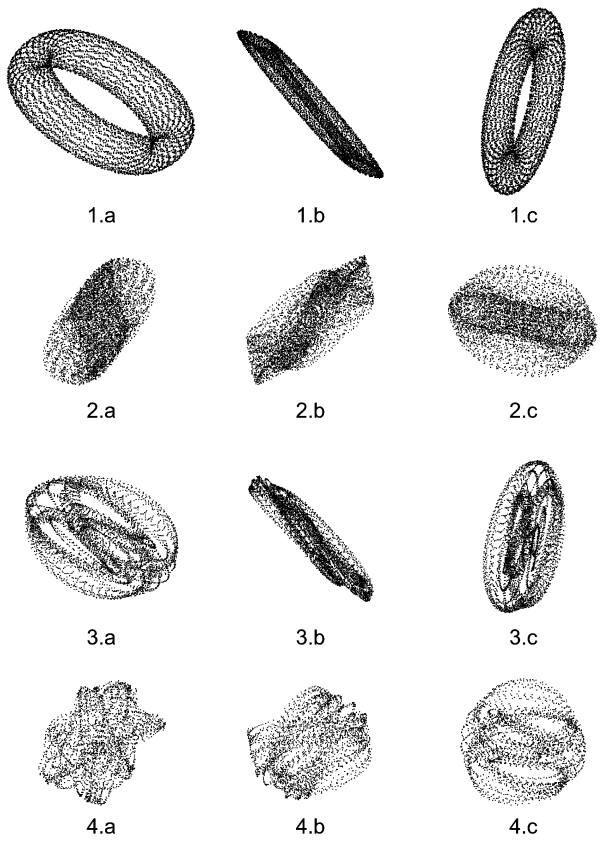

Figure 11: Different visualizations of the state-space in the driven regime with parametric excitation compared to non-parametric regime. First line corresponds to the driven regime without parametric excitation; regular torii are seen. Lag-time for (1.a-c) is 60. Pictures (2.a-4.c) correspond to the driven regime with parametric excitation. Lag-time is equal to: (2.a-c) 60; (3.a-c) 330; (4.a-c) 660. Indices a,b,c correspond to the three different projections of the 3d Shaw-Takens space. Dimension of the Shaw-Takens window is equal to 3. All trajectories calculated for the same initial conditions. General initial position trajectory: $N_0 = 0.8320$, $N_1 = 0.5547$, $N_i = 0$, $i \geq 2$; the system initial state is a mixture of the first two states. Resonance amplitude $A_0 = 0.3$. Parametric excitation $\epsilon = 0.1$, frequency 0.01690 (the last three lines).

We shall use dimensionless units that are convenient for the needs of the numerical simulation.

$$t_R = \nu_S t, \qquad x_R = x/x_0 \tag{4.2}$$

where ν_S and x_0 are the characteristic frequency and the length. The dimensionless expression for energy reads

$$U_R = \frac{\nu_S}{\hbar} U$$

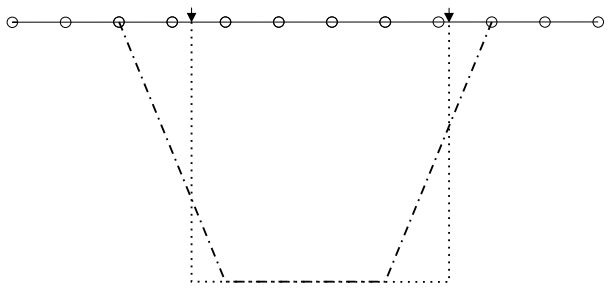

Figure 12: Regularization of potential U with respect to the integration mesh. Bold line gives the initial continuous potential; dashed line indicates potential U_{discr} used in the numerical simulation for the chosen integration step.

Using the dimensionless variables we may cast the Schrödinger equation in the form

$$i\,\frac{\partial}{\partial t_R}\,\psi = -\lambda\frac{\partial^2}{\partial\, x_R^2}\,\psi + U_R\,\psi + V_R(x,t)\,\psi \tag{4.3}$$

where the excitation potential V_R reads

$$V_R = i\,A_R \sin(\Omega_R t_R)$$

The numerical simulation uses the following values of the potential's parameters

$$D = 0.876, \quad L_0 = 2.337, \quad L_1 = 2.045, \quad U_0 = 13.82, \quad U_1 = 11.91$$

chosen in such a way that the discrete part of the spectrum comprises 6 levels

$$E_0 = -12.5998;\ E_1 = -10.4388;\ E_2 = -9.11647;$$
$$E_3 = -6.38743;\ E_4 = -4.06214;\ E_5 = -1.03578.$$

The quasi-classical approximation does not work in this case, since the de Broglie wave-length is comparable with the characteristic size of the system. For the chosen parameters of the well the ground state $|0>$ corresponds to the particle's being almost totally confined to the left part of the well, whereas the first excited level $|1>$ corresponds to its confinement to the right one. Therefore the transitions $|0> \rightleftharpoons |1>$ correspond to the tunneling from one part of the double-well to the other. The circumstance is important for understanding the system's dynamics and one should keep it in mind while considering Figs. 1, 2, and 9.

In what follows the scale frequency ν_S is chosen in such a way that the dimensionless constant λ be equal to 1. If we consider the spatial scale L of the order $3 \cdot 10^{-8}\,cm$ and the mass of the particle $1.8 \cdot 10^{-24}\,g$, we shall have ν_S of the order 50 GHz. The size of the amplitude of the excitation should be of the order 1, that is by an order of magnitude less than the depth of the well.

We preserve on the right hand side of (4.1) all the terms corresponding to $E_0, E_1, ..., E_5$ and neglect the whole continuous spectrum. For the present paper the key point is the observation that the time averages given by (1.2), converge. We made the verification of this statement, see Fig. 13, which indicates that the statement appears to be true. At the same time, it should be noted that besides simple model cases like the motion inside the rectangular well, we do not know any analytical arguments in its favour.

It is important that there is an alternative method of finding numerical solutions to the Schrödinger equation, i.e. the finite difference approximation. For this end we use the Cranck-Nicholson method, [16, 17]. In the case of the rectangular potential the behavior of second derivatives of the wave function at the edges of the well requires special attention, since for long periods of calculation time, or the number of steps, they may generate considerable errors. The difficulty can be overcome, nevertheless, by a regularization procedure. From a formal point of view the Schrödinger equation looks rather similar to the equation of heat conduction, and therefore one could expect that the methods employed for solving numerically the latter, be acceptable for the Schrödinger one. But, it is necessary to take into account the complex structure of the wave equation and its solution, in contrast to the heat equation dealing with real quantities. The circumstance is adequately expressed by the phase of the wave function, which is a source of instabilities peculiar to the quantum phenomena. For example, they are to be accommodated in networks of the Josephson junctions and thus bring out serious difficulties for their use in electronic devices. Nevertheless the numerical methods used for the heat conduction equation are employed for the Schrödinger one, as well. The reason for this is twofold. For one thing, so far, there has been nothing better, and for another they work well enough, at least if one is looking carefully after them. The method widely used is the Cranck-Nicholson one, and its modification the DUFUR method. There is also the fractional step method using the Fourier transform in momentum at every second step of the integration. The Cranck-Nicholson method admits a considerable modification, [16], using recent developments in computer algebra systems such as Maple.

The rectangular barrier studied in this paper has certain advantages even from the computational standpoint, since it admits the explicit calculation of the stationary states. At the same time it presents serious difficulties for analytical treatment, for example, the quasi-classical approximation, owing to its non-differentiable form. The latter may result in fatal errors in the regimes of long-time calculations. Fortunately, a regularization procedure that serves as a cure to the trouble, can be devised .

The primary course of numerical errors due to the rectangular potential is the incompatibility of the integration mesh and the parameters of the continuous initial problem, specifically, the sites of the mesh being out of step with the characteristic points of the potential, see Fig. 12. In fact, the function representing the potential has a discontinuity at point x of the well boundary. This may result in substantial numerical errors. Therefore, we shall choose a discrete form that could mimic a continuous version of the potential and at the same time be acceptable by giving the correct result in the limit of the integration step in x tending to zero. The recipe is as follows: for a given step in x the boundaries of the well are to be adjusted to the sites of the mesh and the parameters of the potential changed in such a way that the discrepancy between

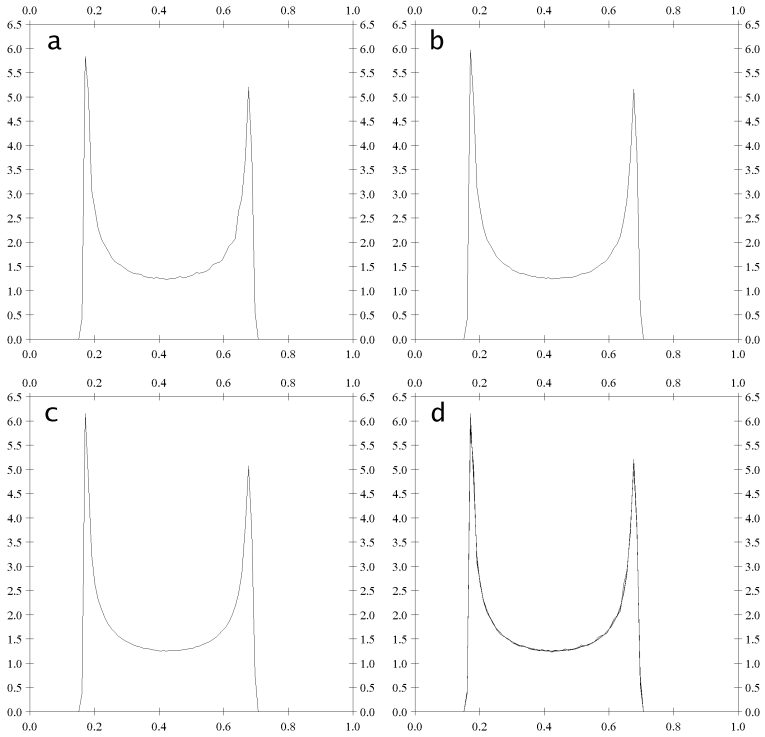

Figure 13: Figs $a-c$ illustrate coarse-grained probability distribution $\rho(N_0)$ calculated by averaging over time periods 15000, 30000, 60000 respectively. In Fig d three distributions a, b, c are plotted together. Resonance amplitude $A_0 = 0.3$, no parametic excitation. General initial position trajectory: $N_0 = 0.8320$, $N_1 = 0.5547$, $N_i = 0$, $i \geq 2$; the system initial state is a mixture of the first two states.

the continuous and the discrete forms of the well disappear.

The main point is the wise adjustment of the discrete form of the well potential. We have chosen the most simple one as shown in Fig. 12.

At this point it should be noted that the resonance value ω_{prm} for the parametric excitation was obtained above by using the rough approximation of rotating wave, and that higher resonant values are to be expected. One may choose the width W of the ring filled by the system trajectory in $N_0-\theta$ plane as a numerical estimate of the effect produced by the parametric pumping. Then, by changing the frequency of the parametric excitation one may find the resonant value as that which corresponds to the maximum of W against ω, see Figs. 5, 6.

So far only the main frequency close to $A_0\kappa_{10}/\hbar$ of the parametric resonance has been considered; higher values of the frequencies are to be expected. We have found the value of frequency $4A_0\kappa_{10}\hbar$ through our calculations with Dirac's equations. Generally, one may expect a multiplet of resonant frequencies, which could have an important bearing on experimental work.

5 Conclusion: Chaotic dynamics due to a non-mono-chromatic pulse

The parametric resonance of the driven tunneling results in the increase in the width of the stripe spanned by the system's trajectory in the 2-dimensional $(N_0 - \theta)$ window on the phase space of Dirac's system. The chaotic dynamics that accompanies it, reveals itself through the peak of the Shannon entropy, $\sigma(\omega)$ which is a function of the modulation frequency.

It is important that the frequency of the resonance parametric excitation ω_{prm} depends on the amplitude A_0 of the driving pulse. In fact, the main resonance frequency is close to

$$\omega_* = \frac{A_0 \kappa_{10}}{\hbar}$$

where κ_{10} is a matrix element determined by the well. It is worth noting that higher resonances are also possible.

The important point is that, for small values of A which are likely to be employed, the values of ω_* are small, and owing to the equation

$$V = \left\{ A_0 \, \sin \Omega t - \frac{A_0}{2} \, \epsilon \, \cos[(\Omega - \omega_*)t] + \frac{A_0}{2} \, \epsilon \, \cos[(\Omega + \omega_*)t] \right\} \, (-i\hbar \frac{\partial}{\partial x})$$

the parametric excitation corresponds to the triplet structure of the pulse V, that is its being determined by the main contribution at frequency $\Omega = (E_1 - E_0)/\hbar$ and two satellites at $\Omega \pm \omega_*$, of less amplitude.

The triplet structure could have an important bearing on the experimental results related to the tunneling in the double-well potential. In fact, if a monochromatic pulse at resonant frequency $\Omega = (E_1 - E_0)/\hbar$ is employed, there is no parametric excitation and the dynamics of the occupation probability has the usual form. In contrast, a poor quality non-monochromatic pulse may contain the triplet indicated above and result in the deformation of the tunneling dynamics.

Acknowledgments

This work was supported by the Grants NS - 1988.2003.1, and RFFI 01-01-00583, 03-02-16173, 04-04-49645.

References

[1] D.T. Monteiro, S.M. Owen, D.S. Saraga, Philos. Trans. Roy. Soc. London Ser. A 357 (1999) 1359.
[2] M. Grifoni, P. Hänggi, Phys. Rep. 304 (1998) 229.
[3] M. Holthaus, Phys. Rev. Lett. 69 (1992) 1596.
[4] M. Büttiker, Phys. Rev. B 27 (1983) 6178.
[5] H.M. Nussenzveig, Phys. Rev. A 62 (2000), 042107.
[6] J.G. Muga, S. Brouard, R. Sala, Phys. Lett. A 167 (1992) 24.

[7] E.H. Hauge, J.A. Stövneng, Rev. Modern Phys. 61 (1989) 917.
[8] P.A.M. Dirac, Proc. Roy. Soc. London Ser. A 114 (1927) 243.
[9] E.T. Jaynes, Phys. Rev. 106 (1957) 620.
[10] M.O. Scully, M.S. Zubairy, Quantum Optics, Cambridge University Press, Cambridge, 1999, Ch. 5.
[11] J.W. Rayleigh, The Theory of Sound, MacMillan, London, 1926, Ch. 3.
[12] R. Bavli, H. Metiu, Phys. Rev. Lett. 69 (1992) 1986.
[13] N.H. Packard, J.P. Crutchfield, J.D. Farmer, R.S. Shaw, Phys. Rev. Lett. 45 (1980) 712.
[14] H.J. Korsch, W. Leyes, New J. Phys. 4 (2002) 62.
[15] B. Mirbach, H.J. Korsch, Phys. Rev. Lett. 75 (1995) 362.
[16] K. Kime, Electron. J. Differential Equations 26 (2000) 1.
[17] S. Yoshida, E. Persson, P. Kristöfel, J. Burgdörfer, Study of the classical-quantum correspondence in a chaotic system, Institut für Theoretische Physik E136, (2003).
[18] K. Ganesan, R. Gębarowski, Pramana — J. Phys.: Special issue - "Nonlinearity and Chaos in the Physical Sciences" 48 (1997) 379.